



Modeling of the oxidation of methyl esters—Validation for methyl hexanoate, methyl heptanoate, and methyl decanoate in a jet stirred reactor

Pierre Alexandre Glaude, Olivier Herbinet, Sarah Bax, Joffrey Biet, Valérie Warth, Frédérique Battin Leclerc

► To cite this version:

Pierre Alexandre Glaude, Olivier Herbinet, Sarah Bax, Joffrey Biet, Valérie Warth, et al.. Modeling of the oxidation of methyl esters—Validation for methyl hexanoate, methyl heptanoate, and methyl decanoate in a jet stirred reactor. *Combustion and Flame*, 2010, 157 (11), pp.2035-2050. 10.1016/j.combustflame.2010.03.012 . hal-00724818

HAL Id: hal-00724818

<https://hal.science/hal-00724818>

Submitted on 22 Aug 2012

HAL is a multi-disciplinary open access archive for the deposit and dissemination of scientific research documents, whether they are published or not. The documents may come from teaching and research institutions in France or abroad, or from public or private research centers.

L'archive ouverte pluridisciplinaire **HAL**, est destinée au dépôt et à la diffusion de documents scientifiques de niveau recherche, publiés ou non, émanant des établissements d'enseignement et de recherche français ou étrangers, des laboratoires publics ou privés.

Modeling of the oxidation of methyl esters—Validation for methyl hexanoate, methyl heptanoate, and methyl decanoate in a jet-stirred reactor

Pierre Alexandre Glaude^a, Olivier Herbinet^{a,*}, Sarah Bax^a, Joffrey Biet^a, Valérie Warth^a and Frédérique Battin-Leclerc^a

^a Laboratoire Réactions et Génie des Procédés, CNRS UPR 3349, Nancy-Université, ENSIC, 1 rue Grandville, BP 20451, 54001 Nancy Cedex, France

Abstract

The modeling of the oxidation of methyl esters was investigated and the specific chemistry, which is due to the presence of the ester group in this class of molecules, is described. New reactions and rate parameters were defined and included in the software EXGAS for the automatic generation of kinetic mechanisms. Models generated with EXGAS were successfully validated against data from the literature (oxidation of methyl hexanoate and methyl heptanoate in a jet-stirred reactor) and a new set of experimental results for methyl decanoate. The oxidation of this last species was investigated in a jet-stirred reactor at temperatures from 500 to 1100 K, including the negative temperature coefficient region, under stoichiometric conditions, at a pressure of 1.06 bar and for a residence time of 1.5 s: more than 30 reaction products, including olefins, unsaturated esters, and cyclic ethers, were quantified and successfully simulated. Flow rate analysis showed that reactions pathways for the oxidation of methyl esters in the low-temperature range are similar to that of alkanes.

Keywords: Methyl esters; Oxidation; Detailed kinetic model; Methyl decanoate; Methyl heptanoate; Methyl hexanoate

Corresponding author : Olivier Herbinet

Laboratoire Réactions et Génie des Procédés, CNRS UPR 3349, Nancy-Université, ENSIC, 1 rue Grandville, BP 20451, 54001 Nancy Cedex, France.

Tel : +33 3 83 17 53 60 ; Fax : +33 3 83 37 81 20

E-mail : olivier.herbinet@ensic.inpl-nancy.fr

1. Introduction

The mitigation of climate change and the impending scarcity of oil resources have led to increasing interest in shifting from hydrocarbon fossil fuels to biofuels (particularly bioethanol and biodiesel [1] and [2]). Since the principal components of plant matter, cellulose and starch, have the molecular formula $(C_6H_{10}O_5)_n$, these new fuels will contain substantial amounts of oxygen, which will have both positive and negative impacts on exhaust emissions: positive—reduction in particulate emissions [3] and [4], negative—increased propensity to form toxic by-products such as aldehydes [5]. Therefore, a deeper understanding of oxygenate biofuel combustion chemistry is necessary to fully exploit positive aspects and minimize negative ones. Unfortunately, there is a clear scarcity of detailed models and kinetic data for oxygenated compounds.

Biodiesel is composed of monoalkyl esters (methyl/ethyl esters) obtained from long-chain fatty acids derived from renewable lipid sources (e.g., rapeseed oil in Europe, soybean oil in the United States, and palm oil in Asia) by transesterification with methanol or ethanol [2] and [6]. Vegetable oils mainly include triglycerides (98%), with small amounts of mono- and di-glycerides. The fatty acid composition of rapeseed oil is 64.4% oleic acid (C18:1 monounsaturated), 22.3% linoleic acid (C18:2 omega-6 polyunsaturated), 8.2% α -linolenic acid (C18:3 omega-3 polyunsaturated), 3.5% of palmitic acid (C16:0 saturated), and 0.9% stearic acid (C18:0 saturated) [6]. Despite that, while several models have been proposed to reproduce the oxidation of methyl butanoate under a wide range of experimental conditions [7], [8], [9], [10], [11] and [12], there is only one model for a heavier methyl ester, methyl decanoate [13]. Due to a lack of relevant experimental data, this detailed mechanism has only been tested for reproducing the oxidation of rapeseed oil methyl esters in a jet-stirred reactor and the ignition delay times of n-decane; only a reduced version of it has been used to model experimental results for the extinction and ignition of methyl decanoate in laminar nonpremixed flows [14].

However, new experimental data are just starting to be available for methyl esters up to C₈. HadjAli et al. [15] have investigated the low-temperature autoignition of methyl esters from C₅ to C₈ in a rapid compression machine and Dayma et al. have studied the oxidation of methyl hexanoate [16] and methyl heptanoate [17] in a jet-stirred reactor.

The purpose of this paper is to describe detailed new kinetic models for the oxidation of methyl esters based on an automatic method of generation and on a single set of kinetic parameters. Validations have been performed using the data obtained by Dayma et al. [16] and [17]. However, to obtain additional reliable data in the low- and intermediate-temperature ranges and to validate the model for a compound heavier than methyl heptanoate, a new experimental study of the oxidation of methyl decanoate was performed in a jet-stirred reactor.

2. Description of the kinetic model

The detailed kinetic mechanisms used in this study have been generated automatically by the computer package EXGAS. This software has already been used for generating mechanisms in the cases of alkanes [18], [19], [20] and [21], ethers [22], and alkenes [23]. We will recall here very briefly its main features, which have already been much described, and we will present the specificities in the reactions and rate constants that were taken in account and implemented in the system to represent the behavior of methyl esters. Note that a first attempt to model the oxidation of methyl esters using EXGAS has already been made in the case of methyl butanoate [12].

2.1. General features of EXGAS

The system provides reaction mechanisms made of three parts:

- A comprehensive primary mechanism, where the only molecular reactants considered are the initial organic compounds and oxygen. According to the choices of the user, the reactant and the primary radicals can be systematically subjected to the following different types of elementary steps:
 - Unimolecular initiations involving the breaking of a C–C bond.
 - Bimolecular initiations with oxygen to produce alkyl and $\text{HO}_2\bullet$ radicals.
 - Oxidations of alkyl radicals with O_2 to form alkenes and $\text{HO}_2\bullet$ radicals.
 - Additions of alkyl ($\text{R}\bullet$) and hydroperoxy-alkyl ($\bullet\text{QOOH}$) radicals to an oxygen molecule.
 - Isomerizations of alkyl and peroxy radicals ($\text{ROO}\bullet$ and $\bullet\text{OOQOOH}$) involving a cyclic transition state; for $\bullet\text{OOQOOH}$ radicals, we consider a direct isomerization–decomposition to give ketohydroperoxides and hydroxyl radicals.
 - Decompositions of radicals by β -scission involving the breaking of C–C or C–O bonds for all types of radicals. Decompositions through the breaking of C–H bonds in ester alkyl radicals are considered if the corresponding option in the “Beta-scissions” section in EXGAS is selected. Note that these reactions are only important at high temperatures.
 - Decompositions of hydroperoxy-alkyl radicals to form cyclic ethers and $\bullet\text{OH}$ radicals.
 - Metatheses involving H-abstractions from the initial reactants by radicals.
 - Combinations of radicals.
 - Disproportionations of peroxyalkyl radicals with $\text{HO}_2\bullet$ to produce hydroperoxides and O_2 (disproportionations between two peroxyalkyl radicals or between peroxyalkyl and alkyl radicals are not taken into account).
- A C_0 – C_2 reaction base, continuously updated, including all the reactions involving radicals or molecules containing less than three carbon atoms [24] and [25]. Two reactions were added to this base in order to take into account the consumption of the radical $\bullet\text{CH}_3\text{OCO}$ ($\bullet\text{C}(=\text{O})\text{-O-CH}_3$), which is specific to the decomposition of methyl esters: $\bullet\text{CH}_3 +$

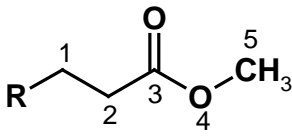
$\text{CO}_2=\bullet\text{CH}_3\text{OCO}$ and $\bullet\text{CH}_3\text{O} + \text{CO}=\bullet\text{CH}_3\text{OCO}$. The kinetic constants of these reactions ($4.76 \times 10^7 \times T^{1.54} \times \exp(-34,700/RT)$ and $1.55 \times 10^6 \times T^{2.02} \times \exp(-5730/RT)$, respectively; units cal, mol, cm^3 , K, s) and the thermodynamic properties of $\bullet\text{CH}_3\text{OCO}$ used in EXGAS were evaluated from ab initio calculations in [26].

- A lumped secondary mechanism, containing the reactions consuming the molecular products of the primary mechanism, which do not react in the reaction base.

To reduce the number of reactants in the secondary mechanism, the molecules with the same molecular formula and the same functional groups formed in the primary mechanism are lumped into one unique species, without distinguishing between the different isomers [18]. The secondary reaction is written to promote the formation of alkyl radicals that contain more than two carbon atoms and that are already included in the primary mechanism [20].

Thermochemical data for molecules or radicals were automatically calculated and stored as 14 polynomial coefficients, according to the CHEMKIN II formalism [27]. These data were automatically calculated using the program THERGAS [28], based on the group and bond additivity methods proposed by Benson [29]. The only change made in the case of esters was the revision of bond dissociation energies of C–H, C–O, and C–C bonds close to the ester function, which were updated from the values recently proposed by El-Nahas et al. [30]. Bond dissociation energies affected by the presence of the ester function are summarized in Table 1.

Table 1. Bond dissociation energies affected by the presence of the ester function.

Position of the bond	Bond energy (kcal/mol)
	
C ₁ -C ₂	83.5
C ₂ -C ₃	93.0
C ₃ -O ₄	97.8
O ₄ -C ₅	85.7
C ₂ -H	94.3
C ₅ -H	99.0

The kinetic data of isomerizations, combinations, and unimolecular decompositions are calculated using the program KINGAS [18], based on thermochemical kinetics methods [29] using the transition state theory or the modified collision theory. The kinetic data that cannot be calculated by KINGAS are estimated from correlations, which are based on quantitative structure–reactivity relationships and obtained from a literature review [19].

2.2. Primary mechanism of the oxidation of methyl esters

The primary mechanisms have been generated using mainly the same rules as those proposed in the case of the oxidation of alkanes [19]. No new specific class of reactions was considered. The following paragraphs describe the changes made in the estimation of kinetic data due to the presence of the ester function:

- Unimolecular initiations by breaking a C–C bond.

The activation energies of unimolecular initiation, which involve the breaking of the C–C bonds located in α - and β -positions from the ester function, have been updated from the bond dissociation energies (equal to 93.0 and 83.5 kcal/mol, respectively) recently calculated by El-Nahas et al. [30]. For the other unimolecular initiations, the bond energies used in THERGAS [28] were in agreement to within about ± 1 kcal/mol with those proposed by El-Nahas et al. [30] and were not modified.

- Bimolecular initiations and metatheses.

Bimolecular initiations and metatheses involve the abstraction of H-atoms from the initial reactant by oxygen molecules or small radicals, respectively. The bond dissociation energy of the C–H bonds carried by the carbon atom just neighboring the ester function (94.3 kcal/mol [30]) is close to that of a tertiary atom of carbon (e.g., 95.7 kcal/mol in isobutene [31]). Thus, for the abstraction of this type of H-atoms, the correlations used are the same as those for the abstraction of tertiary H-atoms from alkanes, except in the case of the abstractions by $\bullet\text{O}\bullet$ and $\bullet\text{H}$ -atoms and by $\bullet\text{OH}$, $\bullet\text{HO}_2$, and $\bullet\text{CH}_3$ radicals. For these last atoms and radicals, the rate parameters have been evaluated using an Evans-Polanyi type correlation proposed by Dean and Bozzelli [32] developed for the abstraction of H-atoms from hydrocarbons,

$k = n_{\text{H}} A T^n \exp\{-[E_0 - f(\Delta H_0 - \Delta H)]/RT\}$, where n_{H} is the number of abstractable H-atoms; A , n , and E_0 are the rate parameters in the case of a metathesis by the considered radical from ethane; ΔH_0 is the enthalpy of the metathesis by the considered radical from ethane; ΔH is the enthalpy of the metathesis by the considered radical from the reacting molecule; and f is a correlation factor, the value of which is given by Dean and Bozzelli [32] for each considered radical.

For the abstraction of an H-atom from the methyl group in the ester function, the correlations used are the same as those for the abstraction of a primary H-atom from alkanes, except in the case of

abstraction by $\bullet\text{O}\bullet$ and $\bullet\text{H}$ -atoms and by $\bullet\text{OH}$, $\bullet\text{HO}_2$, and $\bullet\text{CH}_3$ radicals, the rate parameters of which have also been evaluated using the Evans–Polanyi type correlation from Dean and Bozzelli [32].

- Oxidations of alkyl radicals.

The correlations used for the estimation of kinetic parameters of reactions of oxidation were the same as the ones used in the case of alkanes [19].

- Intramolecular isomerizations of alkyl and alkylperoxy radicals.

As in our previous work [18], the activation energy is set equal to the sum of the activation energy for H-abstraction from the molecule by analogous radicals and the strain energy involved in the cyclic transition state. Some values had to be changed to take into account the influence of the ester group. The activation energy for the internal H-abstraction in α -position from the ester function has been taken as equal to that for the abstraction of a tertiary H-atom in the case of alkanes (i.e., 9 kcal/mol for abstraction by an alkyl radical and 14 kcal/mol for abstraction by an alkylperoxy radical [19]).

The ring strain energy involved in the transition state of some reactions of isomerization, shifting an H-atom above the ester function, also had to be reestimated. These isomerizations concern ester alkyl radicals ($\text{R}\bullet$) and ester alkylperoxy radicals ($\text{RO}_2\bullet$).

The ring strain energies of the transition states involved in the reactions of isomerization of ester alkyl radicals ($\text{R}\bullet$) were deduced from the enthalpies of formation of the corresponding lactones measured by Wiberg and Waldron [33]. Ring strain energies are (in kcal/mol) equal to 9, 11, 11.2, and 12.5 for five-, six-, seven-, and eight-membered ring lactones, respectively.

Isomerizations of alkylperoxy radicals ($\text{RO}_2\bullet$), shifting an H-atom above the ester function, involve cyclic transition states that contain three oxygen atoms. This kind of isomerization occurs through seven- or eight-membered rings, as shown in Fig. 1. Two configurations are possible according to the position of the peroxy group: either the peroxy group is on the alkyl chain and the shifted H-atom is on the methyl group of the ester function, or the peroxy group is on the methyl part of the ester function and the shifted H-atom is on a carbon atom from the alkyl chain. The strain energies have been considered equal to the enthalpies of reaction of the isodesmic reactions yielding the cyclic structure from a linear unstrained one (i.e., reactants and products can be decomposed using the same groups according to the group additivity method of Benson [29]) presented in Fig. 2 in the case

of seven-membered ring species. These enthalpies of reaction have been calculated by quantum methods with the CBS-QB3 composite method implemented in Gaussian03 [34], which leads to a given minimum average deviation of ± 1 kcal/mol for the G2 molecule set. The calculated strain energies are given in Table 2.

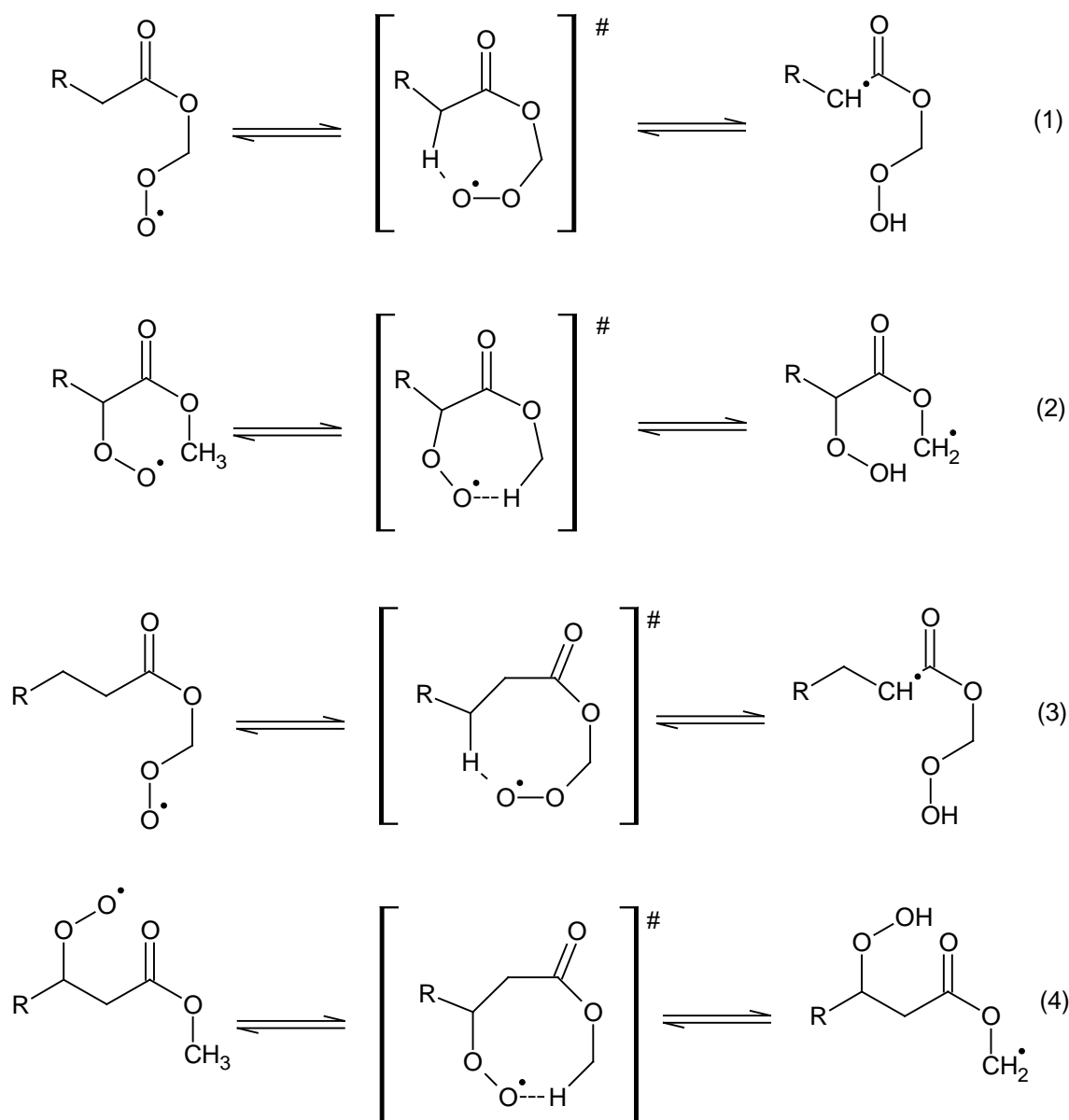


Fig. 1. Reactions of intramolecular isomerization involving transition states including seven- and eight-membered rings containing three oxygen atoms.

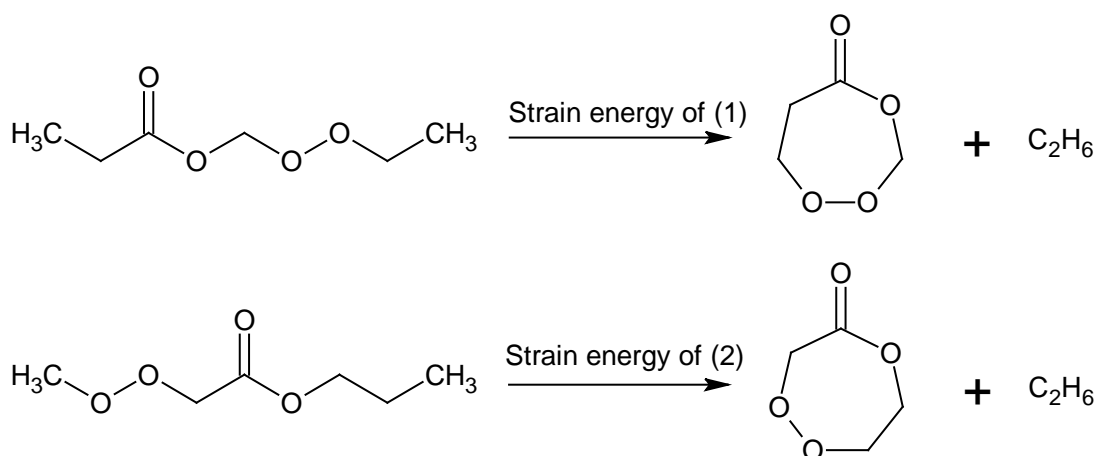


Fig. 2. Isodesmic reactions used to estimate the strain energy of the cyclic transition states involved in the intramolecular isomerizations (1) and (2) in Fig. 1.

Table 2. Strain energies of cyclic transition states involved in reactions of isomerization of ester alkylperoxy radicals (RO₂radical dot) that shift an H-atom above the ester function.

Reaction in Figure 1	Strain energy (kcal/mol)
(1)	8.5
(2)	7.7
(3)	13.6
(4)	9.4

- Decompositions of radicals by β -scission.

The presence of oxygen atoms in the involved radicals can have a significant impact on the values of the activation energies of decomposition by β -scission. Quantum calculations were performed for model reactions at the CBS-QB3 level of theory using Gaussian03 [34]. Intrinsic Reaction Coordinate (IRC) calculations have been systematically performed at the B3LYP/6-31G(d) level of theory on transition states, to ensure that they are correctly connected to the desired reactants and products. Table 3 displays the model reactions that were considered for the calculation and the values that were used for the activation energies of the decompositions of oxygenated radicals by β -scission. To reduce the computational cost, model molecules with short alkyl chains were considered. Only the first and the fifth model reactions could be affected by the choice of the model molecules, as they produced methyl radicals. It is expected that the activation energies would be slightly lower if larger alkyl radicals were produced.

Table 3. Activation energies used for the decompositions by β -scission of oxygenated radicals involved in the oxidation of methyl esters.

Types of reaction	E_a (kcal/mol)
$\text{R}-\overset{\text{O}}{\parallel}{\text{C}}-\text{O}\cdot \longrightarrow \text{R}\cdot + \text{CO}_2 \quad \text{a}$	5.1
$\text{R}-\overset{\text{O}}{\parallel}{\text{C}}-\text{O}-\text{CH}_2\cdot \longrightarrow \text{R}-\overset{\text{O}}{\parallel}{\text{C}}\cdot + \text{CH}_2\text{O} \quad \text{a}$	31.9
$\text{R}-\text{CH}\cdot-\overset{\text{O}}{\parallel}{\text{C}}-\text{O}-\text{CH}_3 \longrightarrow \text{R}-\text{CH}=\text{C}=\text{O} + \text{H}_3\text{C}-\text{O}\cdot \quad \text{b}$	49.0
$\text{R}-\text{CH}\cdot-\text{CH}_2-\overset{\text{O}}{\parallel}{\text{C}}-\text{O}-\text{CH}_3 \longrightarrow \text{R}-\text{CH}=\text{CH}_2 + \text{O}=\text{C}\cdot-\text{O}-\text{CH}_3 \quad \text{b}$	31.2
$\text{R}-\text{CH}_2-\overset{\text{O}}{\parallel}{\text{C}}\cdot \longrightarrow \text{H}_2\text{C}=\text{C}=\text{O} + \text{R}\cdot \quad \text{c}$	39.9
$\text{R}-\text{CH}\cdot-\text{CH}_2-\overset{\text{O}}{\parallel}{\text{C}}-\text{O}-\text{CH}_3 \longrightarrow \text{R}-\text{CH}=\text{CH}-\overset{\text{O}}{\parallel}{\text{C}}-\text{O}-\text{CH}_3 + \text{H}\cdot \quad \text{b}$	34.9

^a The calculation has been performed for $\text{R}\cdot = \text{CH}_3\cdot$.

^b The calculation has been performed for $\text{R}\cdot = \text{H}\cdot$.

^c The calculation has been performed for $\text{R}\cdot = \text{C}_2\text{H}_5\cdot$.

- Additions of radicals to molecular oxygen, decomposition of hydroperoxy-alkyl radicals to cyclic ethers, and decomposition of peroxy-hydroperoxy-alkyl radicals to ketohydroperoxides.

For these classes of reactions, the correlations used for the estimation of the kinetic parameters are the same as the ones used in the case of alkanes [19].

2.3. Secondary mechanism of the oxidation of methyl esters

The primary mechanism for the oxidation of esters leads to the formation of hydroperoxides, cyclic ethers, ketones, and aldehydes bearing an ester function, as well as of unsaturated methyl esters.

New rules have been implemented in EXGAS so that reactions consuming these species are generated. These rules are described in [Table 4], [Table 5], [Table 6], [Table 7] and [Table 8]. The general idea followed to write these rules is the same as that used for the secondary species obtained during the oxidation of alkanes [20]: the formation of radicals, the reactions of which are already included in the primary mechanism (i.e., radicals having more than two carbon atoms), is promoted.

Table 4. Rules for the generation by EXGAS of the reactions of unsaturated methyl esters.

Number of carbon atoms	Obtained products	Rate Parameters
<i>H-abstraction by small radicals for unsaturated methyl esters ($C_nH_{(2n-2)}O_2ZS$)</i>		
n = 4	HCHO + CO + $\bullet C_2H_3$	As for the abstraction of 3 primary alkyl H-atoms from an alkane
n = 5	HCHO + CO + $\bullet C_3H_5$	As for the abstraction of 3 primary alkyl and of 2 secondary allylic H-atoms from an alkane
n ≥ 6	HCHO + CO + $C_4H_6 + \bullet C_{(n-6)}H_{(2n-11)}$	As for the abstraction of 3 primary alkyl H-atoms from an alkane
	$C_4H_6 + \bullet C_{(n-4)}H_{(2n-9)}O_2S$	As for the abstraction of 2 H secondary allylic H-atoms from an alkane
	$\bullet C_2H_3 + C_{(n-2)}H_{(2n-6)}O_2ZS$	As for the abstraction of (2n – 10) secondary alkyl H-atoms from an alkane
<i>Additions on unsaturated methyl esters ($C_nH_{(2n-2)}O_2ZS$)</i>		
$\bullet H$	$\bullet CH_2-C_{(n-1)}H_{(2n-3)}O_2S$	$1.32 \cdot 10^{13} \exp(-1640/T)$
	$CH_3-\bullet CH-C_{(n-2)}H_{(2n-5)}O_2S$	$1.32 \cdot 10^{13} \exp(-785/T)$
$\bullet OH$	$HCHO + \bullet C_{(n-1)}H_{(2n-3)}O_2S$	$2.74 \cdot 10^{12} \exp(520/T)$
$\bullet CH_3$	$C_3H_6 + \bullet C_{(n-2)}H_{(2n-5)}O_2S$	$1.69 \cdot 10^{11} \exp(-3720/T)$
		$9.64 \cdot 10^{10} \exp(-4030/T)$

Notes: Rate constants are given in cm^3, s^{-1}, mol, K . Small radicals involved in H-abstractions are $\bullet H, \bullet OH, HO_2\bullet, \bullet CH_3, CH_3OO\bullet, \bullet C_2H_5$.

Table 5. Rules for the generation by EXGAS of the reactions of acyclic hydroperoxides formed during the oxidation of methyl esters.

Number of carbon atoms	Obtained products	Rate Parameters
<i>Decomposition of hydroperoxide methyl esters ($C_nH_{2n}O_4PS$)</i>		
n is even (n ≥ 4)	$\bullet OH + \bullet C_{(n/2)}H_{(n-1)}O_2S + C_{(n-2)/2}H_{(n-1)}CHO$	$1.5 \cdot 10^{16} \exp(-21640/T)$
n is odd (n ≥ 3)	$\bullet OH + \bullet C_{(n+1)/2}H_nO_2S + C_{(n-3)/2}H_{(n-2)}CHO$	$1.5 \cdot 10^{16} \exp(-21640/T)$
<i>Decomposition of hydroperoxide unsaturated methyl esters ($C_nH_{(2n-2)}O_4PZS$)</i>		
n = 4	HCHO + CO ₂ + $\bullet OH + \bullet C_2H_3$	$1.5 \cdot 10^{16} \exp(-21640/T)$
n ≥ 5	$C_2H_3CHO + \bullet OH + \bullet C_{(n-3)}H_{(2n-7)}O_2S$	$1.5 \cdot 10^{16} \exp(-21640/T)$
<i>Decomposition of ketohydroperoxide methyl esters ($C_nH_{(2n-2)}O_5KPS$)</i>		
n = 3	$\bullet OH + CH_2O + CO_2 + \bullet CHO$	$1.5 \cdot 10^{16} \exp(-21640/T)$
n = 4	$\bullet OH + CO + CH_2O + \bullet CH_3OCO$	$1.5 \cdot 10^{16} \exp(-21640/T)$
n = 5	$\bullet OH + CO + CH_3CHO + \bullet CH_3OCO$	$1.5 \cdot 10^{16} \exp(-21640/T)$
n ≥ 6	n is even $\bullet OH + CO + \bullet C_{(n-2)/2}H_{(n-1)} + C_{n/2}H_{n-2}O_3AS$	$1.5 \cdot 10^{16} \exp(-21640/T)$
	n is odd $\bullet OH + CO + \bullet C_{(n-1)/2}H_n + C_{(n-1)/2}H_{n-3}O_3AS$	$1.5 \cdot 10^{16} \exp(-21640/T)$

Note: Rate constants are given in cm^3, s^{-1}, mol, K .

Table 6. Rules for the generation by EXGAS of the reactions of cyclic ethers formed during the oxidation of methyl esters.

Number of carbon atoms	Obtained products	Rate Parameters
<i>H-abstractions from cyclic ethers with the ester function inside the ring ($C_nH_{(2n-2)}O_3E\#x$)</i>		
$n \geq 4$	$CO_2 + CO + \bullet C_{(n-2)}H_{(2n-3)}$	As for the abstraction of 3 tertiary alkyllic and 2n-5 secondary alkyllic H-atoms from an alkane
<i>H-abstractions from cyclic ethers with the ester function outside the ring ($C_nH_{(2n-2)}O_3E\#xS$)</i>		
$C_nH_{(2n-2)}O_3E\#3S$ and $C_nH_{(2n-2)}O_3E\#xS$, x=4, 5 and 6 which do not have the same skeleton as the reactant	n=4	$\bullet CH_3OCO + CH_2COZ$
	n=5	$\bullet C_3H_5O_2S + CH_2COZ$
	n=6	$\bullet C_3H_5O_2S + C_2H_3CHOZ$
	n=7	$\bullet C_4H_7O_2S + C_2H_3CHOZ$
	n even (n≥8)	$\bullet C_{(n/2)}H_{(n-1)}O_2S + C_{n/2}H_{(n-2)}OKZ$
	n odd (n≥9)	$\bullet C_{(n+1)/2}H_nO_2S + C_{(n-1)/2}H_{(n-3)}OKZ$
$C_nH_{(2n-2)}O_3E\#xS$, x=4, 5 and 6 which have the same skeleton as the reactant	$\bullet C_nH_{2n-3}O_3E\#xS$	As for the abstraction of 3 primary alkyllic and 2n-5 secondary H-atoms from an alkane

Notes: Rate constants are given in cm^3, s^{-1} , mol, K. Small radicals involved in H-abstractions are $\bullet H$, $\bullet OH$, $HO_2\bullet$, $\bullet CH_3$, $CH_3O_2\bullet$, $\bullet C_2H_5$.

Table 7. Rules for the consumption in EXGAS of the radicals obtained from the H-atom abstraction from four-, five-, and six-membered ring cyclic ethers (ester function outside the ring).

Number of carbon atoms	Obtained products	Rate Parameters
<i>Decompositions of ester cyclo-ether radicals ($\bullet C_nH_{(2n-3)}O_3E\#xS$)</i>		
n = 5	$\bullet CHO + C_4H_6O_2S$	$5.0 \times 10^{13} \exp(-12480/T)$
n ≥ 6	$\bullet CH_2CHO + C_{(n-2)}H_{(2n-6)}O_2S$	$5.0 \times 10^{13} \exp(-12480/T)$
<i>Addition of ester cyclo-ether radicals ($\bullet C_nH_{(2n-3)}O_3E\#xS$) to O_2, only if x > 3</i>		
n ≥ 5	$\bullet C_nH_{(2n-3)}O_5E\#xUS$	forward: $3.0 \times 10^{19} T^{-2.5}$ reverse: $5.0 \times 10^{22} T^{-2.5} \exp(-20131/T)$
<i>Isomerisation of peroxy ester cyclo-ether radicals ($\bullet C_nH_{(2n-3)}O_5E\#xUS$)</i>		
n ≥ 5	$\bullet C_nH_{(2n-3)}O_5E\#xPS$	forward: $8.0 \times 10^{13} \exp(-12833/T)$ reverse: $4.8 \times 10^{12} \exp(-9562/T)$
<i>Addition of hydroperoxide ester cyclo-ether radicals ($\bullet C_nH_{(2n-3)}O_5E\#xPS$) to O_2, only if x > 3</i>		
n ≥ 5	$\bullet C_nH_{(2n-3)}O_7E\#xUPS$	forward: $3.0 \times 10^{19} T^{-2.5}$ reverse: $5.0 \times 10^{22} T^{-2.5} \exp(-20131/T)$
<i>Decomposition of peroxy hydroperoxide ester cyclo-ether radicals ($\bullet C_nH_{(2n-3)}O_7E\#xUPS$)</i>		
n ≥ 5	$\bullet OH + C_nH_{(2n-4)}O_6E\#xKPS$	$1.0 \times 10^9 \exp(-3770/T)$
<i>Decompositions of ketohydroperoxide ester cyclo-ether ($C_nH_{(2n-4)}O_6E\#xKPS$)</i>		
n = 5	$\bullet OH + \bullet CH_3 + CH_2CO + 2 CO_2$	$1.5 \times 10^{16} \exp(-12480/T)$
n ≥ 6	$\bullet OH + CO_2 + \bullet CHO + C_{(n-2)}H_{(2n-6)}O_2S$	$1.5 \times 10^{16} \exp(-12480/T)$

Note: Rate constants are given in cm^3, s^{-1} , mol, K.

Table 8. Rules for the generation by EXGAS of the reactions of ketones and aldehydes formed during the oxidation of methyl esters.

Number of carbon atoms	Obtained products	Rate Parameters
<i>H-abstraction by small radicals for ester with aldehyde function ($C_nH_{(2n-2)}O_3AS$)</i>		
$n \geq 4$	$CO + \bullet C_{(n-1)}H_{(2n-3)}O_2S$	As for the abstraction of 3 primary alkyl H-atoms from an alkane
	$CO + \bullet C_{(n-1)}H_{(2n-3)}O_2S$	As for the abstraction of $(2n-6)$ secondary alkyl H-atoms from an alkane
	$CO + \bullet C_{(n-1)}H_{(2n-3)}O_2S$	As for the abstraction of 1 aldehydic H-atoms from an alkane
<i>H-abstraction by small radicals for ester with ketone function ($C_nH_{(2n-2)}O_3KS$)</i>		
$n \geq 4$	$CH_2CO + \bullet C_{(n-2)}H_{(2n-5)}O_2S$	As for the abstraction of 6 primary alkyl H-atoms from an alkane
	$CH_2CO + \bullet C_{(n-2)}H_{(2n-5)}O_2S$	As for the abstraction of $(2n-8)$ H secondary alkyl H-atoms from an alkane

Note: Small radicals involved in H-abstractions are $\bullet H$, $\bullet OH$, $HO_2\bullet$, $\bullet CH_3$, $CH_3O_2\bullet$, $\bullet C_2H_5$.

To identify the nature of the functions in the species formed in the models generated using EXGAS, some letters are added at the end of their names. The letter S is for an ester function, Z for one C=C double bond, K for a ketone function, A for an aldehyde function, P for a hydroperoxy function, U for a peroxy function, and L for an alcohol function. Cyclic ethers are identified by the letter E (for ether) and the symbol #x, which means that it is a cyclic molecule in which the ring includes x atoms. As an example, all unsaturated methyl esters with n carbon atoms and one double bond will be denoted $C_nH_{2n}O_2ZS$ in the models.

The secondary reactions that were considered in the case of unsaturated esters are H-atom abstractions and the addition of small radicals to the double bond. The rules for the generation of these reactions are summarized in Table 4. As far as H-atom abstractions are concerned, two particular cases are considered for unsaturated esters having four and five atoms of carbon and a general rule was developed for species having at least six atoms of carbon. For the choice of the reaction products and the choice of the nature of the H-atoms which can be abstracted, it was considered that the prevalent unsaturated ester is the one with the double bond at the extremity of the chain (obtained from the decomposition of ester alkyl radicals). In the case of unsaturated species having at least six carbon atoms ($n \geq 6$), three different channels of decomposition were considered according to the location of the abstracted H-atoms. Since these molecules are formed in the primary mechanism by radical decomposition, it is also assumed that the double bond is at the end of the alkyl chain and that these species involve three primary alkyl, two secondary allylic, and $2n - 10$ secondary alkyl H-atoms, the three vinylic H-atoms being neglected. The abstraction of the three primary alkyl H-atoms by Radical dot leads to a molecule RH and a new radical the decomposition of which is directly written to formaldehyde, carbon monoxide, butadiene, and an alkyl radical $\bullet C_{(n-6)}H_{(2n-11)}$ (note that $\bullet C_{(n-6)}H_{(2n-11)}$ is an H-atom if $n = 6$). The abstraction of the two secondary allylic H-atoms by $R\bullet$ leads to a molecule RH and a new radical the decomposition of which is directly written to butadiene and an ester alkyl radical $\bullet C_{(n-4)}H_{(2n-9)}O_2S$ (note that

•C_(n-4)H_(2n-9)O₂S is the radical •CH₃OCO if n = 6). The abstraction of the 2nth secondary alkyl H-atoms by R• leads to a molecule RH and a new radical the decomposition of which is directly written to an unsaturated ester C_(n-2)H_(2n-6)O₂ZS with n – 2 carbon atoms and a radical •C₂H₃.

Reactions of addition of H-atoms and of hydroxyl and methyl radicals to unsaturated esters were also considered (Table 4). The addition of H-atoms leads to the formation of two ester alkyl radicals (H-atoms can add to the two carbon atoms of the double bond), the reactions of which are already considered in the primary mechanism. The addition of an •OH radical to a C_nH_{2n}O₂ZS unsaturated ester and the decomposition of the adduct is considered to occur into one single step which produces a molecule of formaldehyde and a smaller •C_(n-1)H_(2n-3)O₂S radical already present in the primary mechanism. The addition of •CH₃ radicals to a C_nH_{2n}O₂ZS unsaturated ester and the decomposition of the adduct are also considered in one step that produces a molecule of propene and a •C_(n-2)H_(2n-5)O₂S radical already included in the primary mechanism. Two sets of kinetic parameters are used for the addition of H-atoms and methyl radicals in order to take in account the two possible locations for the addition. The kinetic parameters used in the case of the additions of •OH radicals also take into account the possibility of addition on both sides of the double bond.

Table 5 displays the rule of consumption in EXGAS of hydroperoxide species formed during the oxidation of methyl esters. The rule that we considered for the decomposition of this type of species is the breaking of the O–OH bond leading to the formation of an •OH radical and of an alkoxy radical the decomposition of which is directly written into an aldehyde and an alkyl radical bearing an ester function.

The decomposition of hydroperoxide methyl esters (C_nH_{2n}O₄PS) leads to the formation of a C_{(n-2)/2}H_(n-1)CHO aldehyde, an •OH radical, and a C_(n/2)H_(n-1)O₂S ester alkyl radical if n is even (n ≥ 4) and of a C_{(n-3)/2}H_(n-2)CHO aldehyde, an •OH radical, and a •C_{(n+1)/2}H_nO₂S ester alkyl radical if n is odd (n ≥ 3). The decomposition of hydroperoxide unsaturated methyl esters (C_nH_(2n-2)O₄PZS) leads to the formation of acrolein (C₂H₃CHO), an •OH radical, and a •C_(n-3)H_(2n-7)O₂S ester alkyl radical if n ≥ 5 (there is a particular rule for n = 4). For the decomposition of ketohydroperoxide methyl esters (C_nH_(2n-2)O₅KPS), particular rules were developed for species having three, four, and five carbon atoms and a general rule was established for n ≥ 6. For n ≥ 6, the decomposition leads to carbon monoxide, a C_{n/2}H_{n-2}O₃AS aldehyde, and •OH and •C_{(n-2)/2}H_(n-1) radicals if n is even, and to carbon monoxide, a C_{(n-1)/2}H_{n-3}O₃AS aldehyde, and •OH and •C_{(n-1)/2}H_n radicals if n is odd. The kinetic constant used for all these reactions is the one used for the reaction of breaking of the O–OH bond: 1.5 × 10¹⁶ × exp(–43,000/RT) (units cal, mol, cm³, s, K).

As distinguished in Table 6, two types of cyclic ethers can be obtained during the oxidation of methyl esters, ethers with the ester function included in the ring, and ethers with the ester function outside the ring. A cyclic ether with the ester function included in the ring, having n carbon atoms, and having x atoms included in the ether ring is denoted C_nH_(2n-2)O₃ES#x in the models. If the ester

function is outside the ring, the species is denoted $C_nH_{(2n-2)}O_3E\#xS$ (the position of the letter S is different). Note that only five- and six-membered ring cyclic ethers (#5 and #6) are considered if the ester function is included in the ring.

The secondary reactions that were considered for both types of cyclic ethers are H-atom abstractions, but the fate of the radicals obtained depends on the location of the ester function (inside or outside the ring), and on the number of atoms included in the ether ring (Table 6).

The H-atom abstractions from a cyclic ether with the ester function included in the ring ($C_nH_{(2n-2)}O_3ES\#x$) by a radical $R\bullet$ were considered in a simple way: they lead to a molecule RH and a new radical that decomposes directly to carbon monoxide, carbon dioxide, and an alkyl radical $RC_{(n-2)}H_{(2n-3)}$ that is already included in the primary mechanism. It is assumed that the species has three tertiary alkyl and $2n - 5$ secondary alkyl H-atoms.

If the ester function is outside the ring, the rules of generation depend on the number of atoms in the ring. The abstraction of H-atoms from three-membered ring cyclic ethers ($C_nH_{(2n-2)}O_3E\#3S$) by $R\bullet$ leads to a molecule RH and a radical that decomposes directly to a radical already included in the primary mechanism and a ketene, as indicated in Table 6. It is assumed that three primary alkyl and $2n - 5$ secondary alkyl H-atoms are abstracted through these reactions. The four-, five-, and six-membered ring cyclic ethers that do not have the same skeleton as the reactant react the same way as the three-membered ring cyclic ethers, whereas the four-, five-, and six-membered ring cyclic ethers that have the same skeleton as the reactant produce a $\bullet C_nH_{2n-3}O_3E\#xS$ radical by H-abstraction by $R\bullet$, leading to a molecule RH and a $\bullet C_nH_{2n-3}O_3E\#xS$ lumped radical. It is also assumed that three primary alkyl and $2n - 5$ secondary alkyl H-atoms are abstracted through these reactions. The $\bullet C_nH_{2n-3}O_3E\#xS$ radicals (coming from H-atom abstraction from the four-, five-, and six-membered ring cyclic ethers with the ester function outside the ring) react first through reactions of decomposition, leading to the formation of $C_4H_6O_2S$ and $\bullet CHO$ if $n = 5$ or to $C_{(n-2)}H_{(2n-6)}O_2S$ and $\bullet CH_2CHO$ if $n \geq 6$ (Table 7). These $\bullet C_nH_{2n-3}O_3E\#xS$ radicals also play a role in the low-temperature chain branching and the sequence of reactions leading to this chain branching was taken into account: first additions to molecular oxygen yielding peroxy ester cycloether radicals ($\bullet C_nH_{(2n-3)}O_5E\#xUS$), isomerizations of peroxy ester cycloether radicals to hydroperoxide ester cycloether radicals ($\bullet C_nH_{(2n-3)}O_5E\#xPS$), second additions of hydroperoxide ester cycloether radicals to molecular oxygen ($\bullet C_nH_{(2n-3)}O_7E\#xUPS$), decompositions of hydroperoxide ester cycloether radicals to ketohydroperoxide ester cycloether molecules ($\bullet C_nH_{(2n-4)}O_6E\#xKPS$) plus $\bullet OH$, and decompositions of ketohydroperoxide ester cycloether molecules. The kinetic parameters associated with these reactions are summarized in Table 7.

The only secondary reactions considered for aldehydes and ketones with an ester function are H-atom abstractions. The rules for the generation of these reactions are displayed in Table 8. As there is no particular case, only general rules were developed (these species have a minimum of four

carbon atoms). H-atom abstraction from an aldehyde with an ester function and having n atoms of carbon (denoted $C_nH_{(2n-2)}O_3AS$ in the models) by a radical $R\bullet$ leads to a molecule RH and a new radical that is not written and that is considered as rapidly decomposing to give a carbon monoxide molecule and an alkyl ester radical $\bullet C_{(n-1)}H_{(2n-5)}O_2S$ that is already present in the primary mechanism. Note that the reaction is written in a duplicate way in order to take into account the nature of the different H-atoms that are abstracted (a $C_nH_{(2n-2)}O_3AS$ species has three primary, $2n-6$ secondary, and one aldehydic H-atoms). As for aldehydes, H-atom abstraction from a ketone also having an ester function and n atoms of carbon (denoted $C_nH_{(2n-2)}O_3KS$ in the models) by a radical $R\bullet$ leads to a molecule RH and a new radical that is not written and that is considered as rapidly decomposing to give a ketene molecule (CH_2CO) and an alkyl ester radical $\bullet C_{(n-2)}H_{(2n-5)}O_2S$ that is already included in the primary mechanism. This reaction is also written in a duplicate way (a $C_nH_{(2n-2)}O_3KS$ species has six primary and $2n-8$ secondary H-atoms).

3. Experimental and modeling study of the oxidation of methyl decanoate

To validate the models generated using EXGAS for esters up to methyl decanoate, computed results were compared to a new set of methyl decanoate experimental results obtained in a jet-stirred reactor. The new experimental results are presented and simulations computed with the model generated with EXGAS are then compared to them.

3.1. Experimental study of the oxidation of methyl decanoate in a jet-stirred reactor

The oxidation of methyl decanoate ($C_{11}H_{22}O_2$) was performed in a jet-stirred reactor operated at a constant pressure of 1.06 bar, at a residence time of 1.5 s, at temperatures ranging from 500 to 1100 K, and under stoichiometric conditions. The fuel was diluted in helium (fuel mole fraction 0.0021). The jet-stirred reactor is a very convenient device that was used for numerous gas phase studies in our laboratory [12], [20] and [35]. Since the apparatus and the analytical methods used in this work were already described in previous papers on the experimental study of very large methyl esters (methyl palmitate [35] and methyl oleate [36]), we will repeat here only the main features.

The reactor, made of fused silica, consists of a quartz sphere (volume 92 cm³) into which diluted reactant enters through an injection cross located at its center. It is operated at constant temperature and pressure and it is preceded by an annular preheating zone in which the temperature of the gases is increased up to the reactor temperature before entering inside. Gas mixture residence time inside the annular preheater is very short compared to its residence time inside the reactor (a few percent). Both the spherical reactor and the annular preheating zone are heated by heating resistances rolled up around their walls.

Reaction products with five or less heavy atoms (carbon and oxygen atoms) were analyzed online by two gas chromatographs. The first gas chromatograph, equipped with a Carbosphere packed column, a thermal conductivity detector (TCD), and a flame ionization detector (FID), was used for the quantification of O₂, CO, CO₂, and methane. The second gas chromatograph was fitted with a Plot Q capillary column and a FID and was used for the quantification of the following species: acetylene, ethylene, ethane, propene, propane, acetaldehyde, 1,3-butadiene, 1-butene, 1-pentene, and the sum of propanal and acrolein, which could not be separated. Reaction products with more than five heavy atoms were condensed in a trap located at the outlet of the reactor and maintained at the temperature of liquid nitrogen. The content of the trap was then analyzed by a third gas chromatograph equipped with an HP-5 capillary column and a FID. Identification of species was performed with a gas chromatograph (using the same type of column) coupled with a mass spectrometer. The method of the internal standard (n-octane here) was used for the quantification. The mass spectra of most reaction products were included in the spectra database "NBS75 K." For other products, which were not in the database, the deciphering of the mass spectra was carried out. These products were cyclic ethers formed at low temperature and unsaturated esters formed at high temperature. The relative uncertainties have been estimated to be $\pm 5\%$ for species that are analyzed online and $\pm 10\%$ for species that were first condensed in the trap and then analyzed.

Analyzed species were large 1-olefins from 1-hexene to 1-nonene (smaller 1-olefins are analyzed online), unsaturated esters with the double bond at the end of the chain (methyl 2-propenoate, methyl 3-butenate, methyl 5-hexenoate, methyl 6-heptenoate, methyl 7-octenoate, and methyl 8-nonenoate), and numerous C₁₁ cyclic ethers. Methyl 4-pentenoate could not be quantified because its peak was interfering with the large peak of the internal standard (n-octane). Fig. 3 displays an extract of chromatogram showing the peaks of the five-membered ring C₁₁ cyclic ethers. Some of them were not well separated (due to the closeness of their structures; see Table 9) and could not be quantified separately. Note that most cyclic ethers were present twice in the chromatogram in Fig. 3 because of the possible cis/trans isomers when the cyclic ether has two side chains [35]. It is also interesting to note that the cyclic ethers with the ring in the α position of the ester function (species F and F' in Table 9) were not observed in these experiments. Note that the corresponding cyclic ethers were present in very low amounts (close to the limit of detection) in a previous n-decane/methyl palmitate blend oxidation study [35]. The other peaks in Fig. 3 correspond certainly to other C₁₁ oxygenated products, such as other cyclic ethers, ketones, or aldehydes, but it was not possible to identify them. The knowledge of the rules of fragmentation forming the main larger fragments in electronic impact mass spectrometry for five-membered ring cyclic ethers, which had been gained from the study of the oxidation of n-decane [35], has been used for identifying cyclic ethers in the present study.

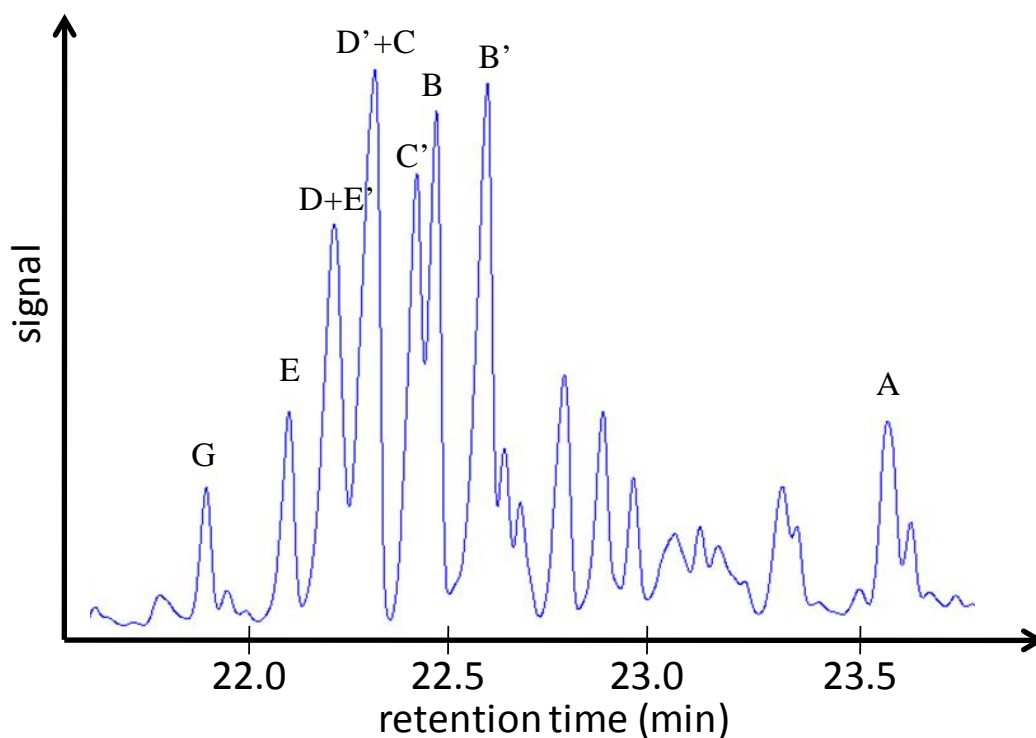
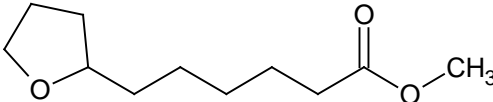
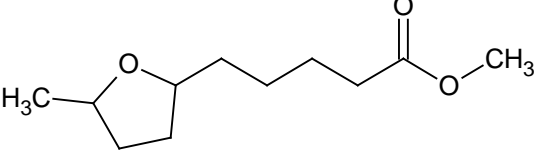
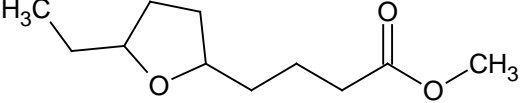
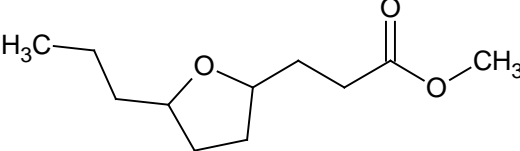
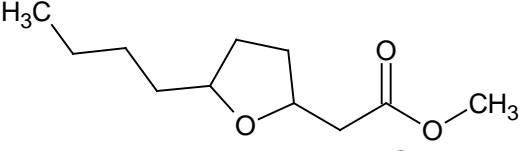
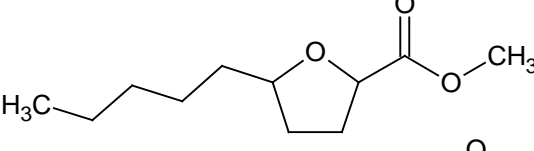
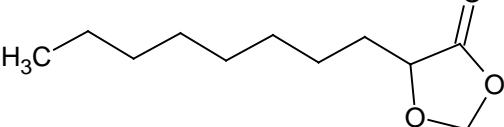


Fig. 3. Extract of a chromatogram showing the peaks corresponding to the cyclic ethers formed in the low-temperature oxidation of methyl decanoate. Letters in the chromatogram refer to the species in Table 9.

The evolution of the conversion of methyl decanoate and of the mole fraction profiles of the reaction products and O_2 are displayed in [Fig. 4], [Fig. 5] and [Fig. 6]. The mole fraction profile of methyl decanoate exhibits strong negative temperature coefficient (NTC) behavior, as can be observed in Fig. 4. The conversion of the reactant reaches 0.63 at 650 K and falls to 0.11 at 800 K. Note that the fuel is still slightly reactive in the temperature range 750–800 K as the formation of small amounts of oxygenated species (such as cyclic ethers) is observed (Fig. 6). Mole fraction profiles of Fig. 6 also show that cyclic ethers are still formed at temperatures following the NTC region and that they disappear at temperatures greater than 900 K. 1-Olefins and unsaturated esters are observed at both low and high temperatures. Note that the mole fraction peak at low temperature of these products decreases when the size of the species increases as it can be observed for 1-olefins from ethylene to 1-nonene and for unsaturated esters from methyl 2-propenoate to methyl 8-nonenoate.

Table 9. Names and structures of the five-membered ring cyclic ethers the formation of which is expected in the low-temperature oxidation of methyl decanoate.

Letter in the chromatogram of Figure 3	Name	Structure	Name in the model
A	2-methyl hexanoate, tetrahydrofuran		M9C11H20O3
B and B'	2-methyl,5-methyl pentanoate, tetrahydrofuran ^a		M31C11H20O3
C and C'	2-ethyl,5-methyl butanoate, tetrahydrofuran ^a		M27C11H20O3
D and D'	2-propyl,5-methyl propanoate, tetrahydrofuran ^a		M23C11H20O3
E and E'	2-butyl,5-methyl ethanoate, tetrahydrofuran ^a		M19C11H20O3
F and F' (not observed)	2-pentyl,5-methyl methanoate, tetrahydrofuran		M15C11H20O3
G	3-octyl,1,4-dioxola-2-one		M11C11H20O3

^a Two isomers (cis and trans) have been detected (see chromatogram in Fig. 3).

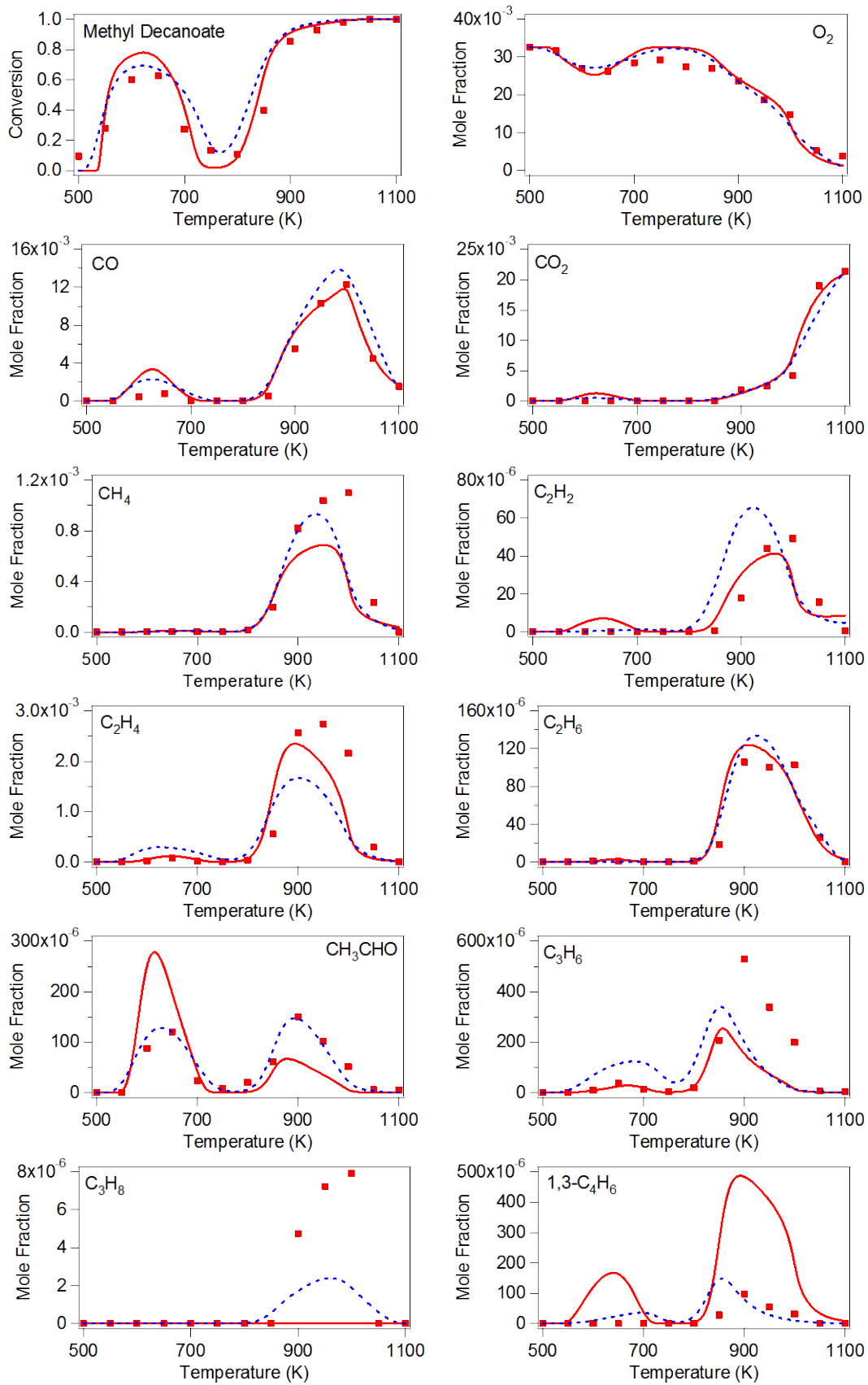


Fig. 4. Oxidation of methyl decanoate in a jet-stirred reactor: comparison of the models (solid line: EXGAS model; broken line: LLNL model [13]) with the new experimental results presented in this paper (pressure: 1.06 bar, equivalence ratio: 1, inlet fuel mole fraction: 0.0021, and residence time: 1.5 s). Part one.

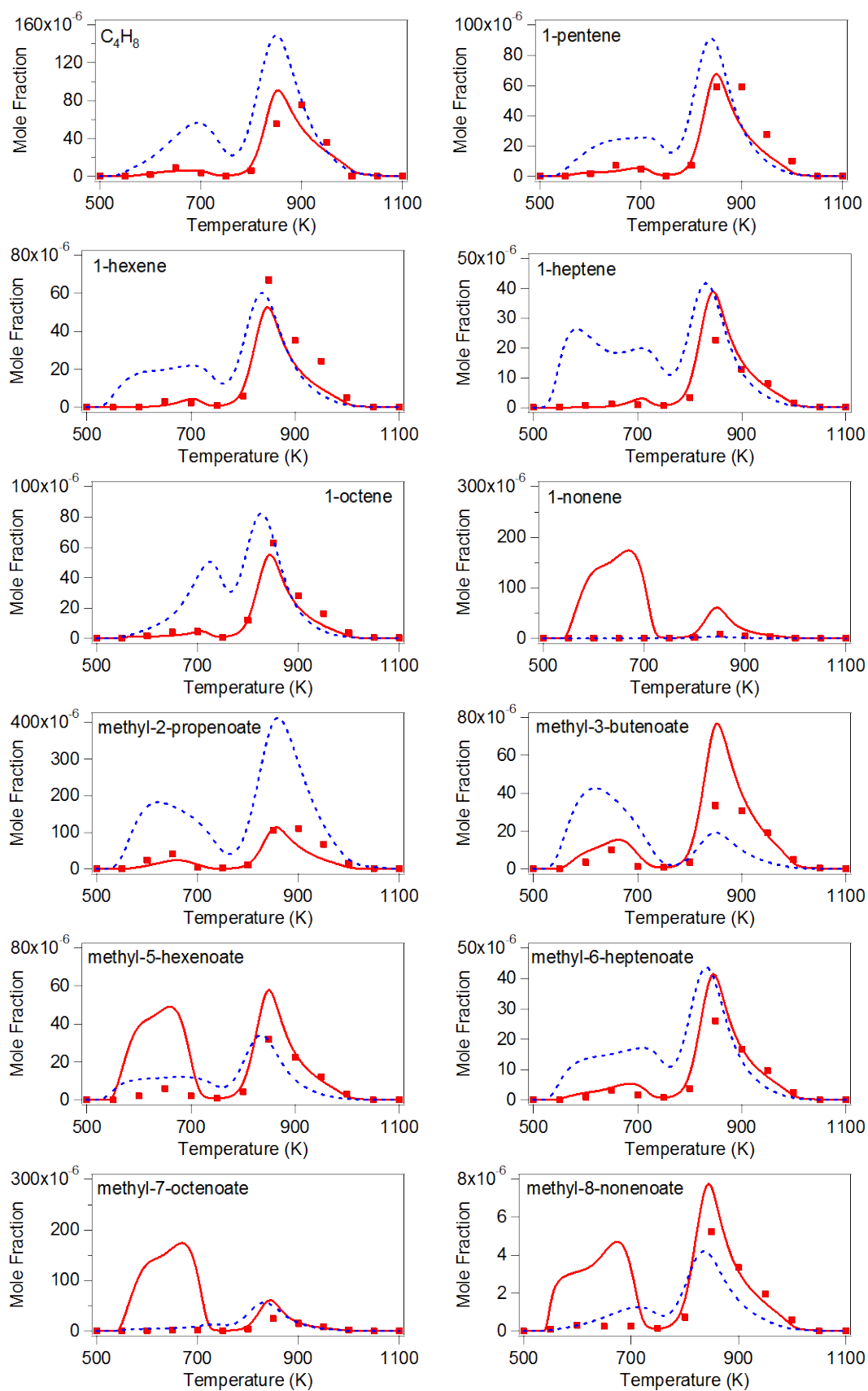


Fig. 5. Oxidation of methyl decanoate in a jet-stirred reactor: comparison of the models (solid line: EXGAS model; broken line: LLNL model [13]) with the new experimental results presented in this paper (pressure: 1.06 bar, equivalence ratio: 1, inlet fuel mole fraction: 0.0021, and residence time: 1.5 s). Part two.

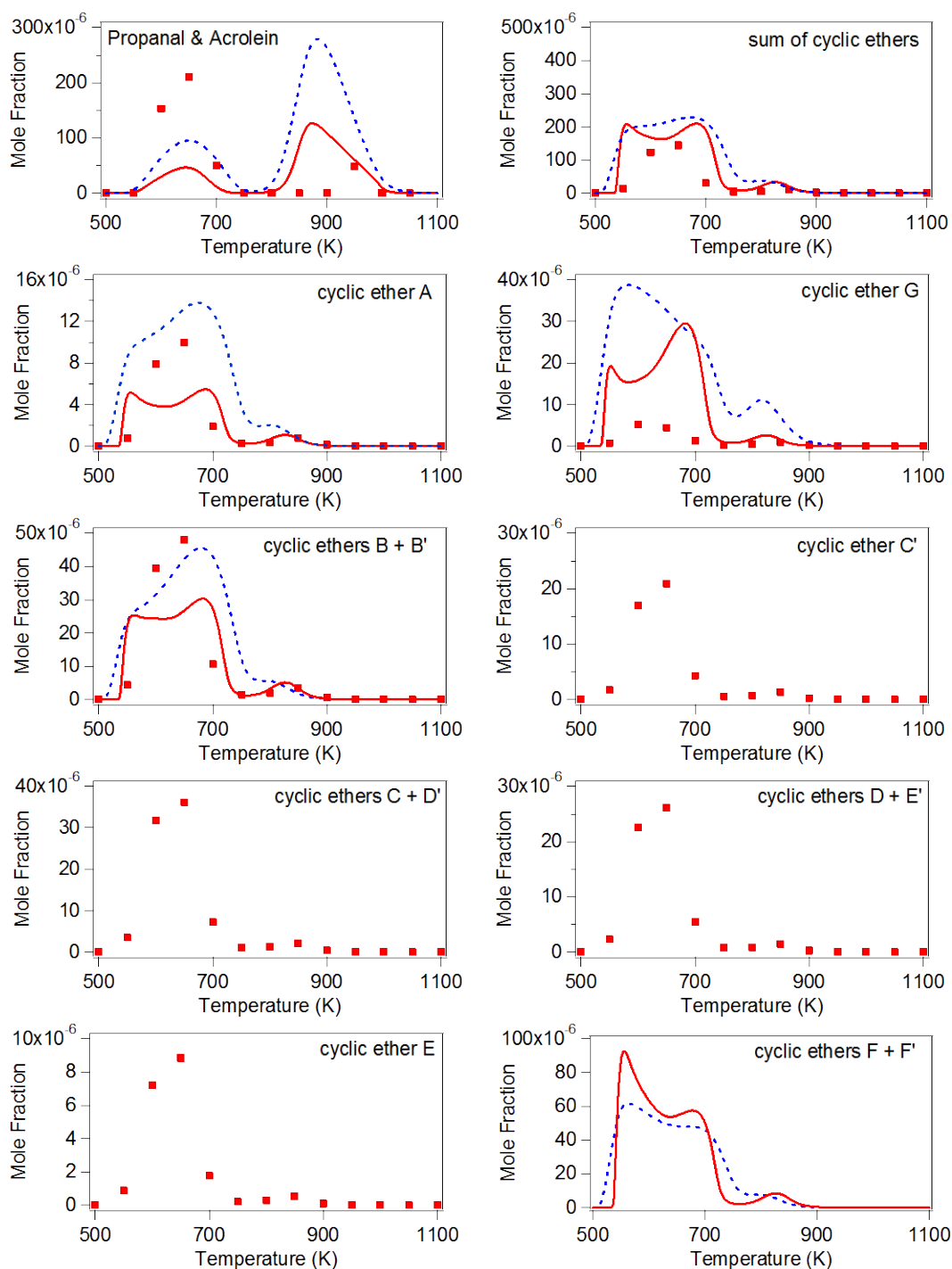


Fig. 6. Oxidation of methyl decanoate in a jet-stirred reactor: comparison of the models (solid line: EXGAS model; broken line: LLNL model [13]) with the new experimental results presented in this paper (pressure: 1.06 bar, equivalence ratio: 1, inlet fuel mole fraction: 0.0021, and residence time: 1.5 s). Part three.

3.2. Modeling of the oxidation of methyl decanoate in a jet-stirred reactor

The detailed kinetic model generated for the oxidation of methyl decanoate is available as Supplementary material (Appendix) of this paper. It globally contains 7171 reactions (462 reactions are in the reactions bases, 4898 in the primary, and 1811 in the secondary mechanisms) involving 1251 species. Simulations were performed using software PSR of CHEMKIN II [27] and assuming homogeneous isothermal reactor. Throughout this part, symbols are experimental data and lines refer to simulations.

Simulations using the methyl decanoate model generated with EXGAS were compared with these new experimental results ([Fig. 4], [Fig. 5] and [Fig. 6]). Note that the kinetic parameters used in this model are those presented in the modeling section of this paper and that none of them was adjusted to obtain better agreement between computed and experimental data. As far as the reactivity is concerned, the model reproduces well the conversion of the fuel and the mole fraction of oxygen. The NTC behavior is well predicted with still a slight reactivity in the range 750–800 K. Computed mole fractions of the main reaction products, such as CO and CO₂, are in very good agreement with experimental data. As far as 1-olefins and unsaturated esters are concerned, the agreement is overall satisfactory with some discrepancies for some species such as 1-nonene, methyl 5-hexenoate, methyl 7-heptenoate, and methyl 8-octenoate, which are overestimated at low temperature. The prediction of the mole fractions of methane, acetylene, ethane, and acetaldehyde is relatively correct, whereas the formation of propane is underestimated and that of 1,3-butadiene is overestimated. The production of the sum of propanal and acrolein is underestimated below 800 K and overestimated for higher temperatures.

The sum of five-membered ring C₁₁ cyclic ethers is well captured by the model. The fact that three maxima are observed in the simulated profile is due to two concurrent impacts of the enhanced reversibility of the addition of alkyl and hydroperoxyalkyl radicals to oxygen: the decrease of the reactivity, which is the origin of the NTC behavior, and the favored formation of cyclic ethers from hydroperoxyalkyl radicals. In the models generated with EXGAS, the cyclic ethers having the same global formula are usually lumped into one species whereas we were able to distinguish between the different isomers in the experiments. For the present validation, the code in EXGAS was modified in order to distinguish between the different C₁₁ cyclic ethers in the model. However, the simulated profiles of three cyclic ethers (C, D, and E in Table 9) could not be compared to the experimental ones, because their corresponding peaks were not well separated (see Fig. 3).

4. Modeling study of the oxidation of methyl hexanoate and heptanoate

Dayma et al. [16] studied the oxidation of methyl hexanoate ($C_7H_{14}O_2$) in a jet-stirred reactor operated at a pressure of 10 atm, a residence time of 1 s, over the temperature range 500–1000 K, and at high dilution in nitrogen. The inlet fuel mole fraction was 0.001 and three equivalence ratios were investigated: 0.5, 1, and 1.5. Reaction products were analyzed by gas chromatography. Species quantified in this study (not all species were quantified for every equivalence ratio) were oxygen, hydrogen, carbon monoxide, carbon dioxide, formaldehyde, methane, acetaldehyde, ethane, ethene, acetylene, propene, propanal, propenal, 1-butene, 1-pentene, and unsaturated methyl esters from C_4 to C_7 . No cyclic ether was analyzed.

A model for the oxidation of methyl hexanoate (401 species and 2440 reactions) has been generated by the version of EXGAS described in this paper. [Fig. 7] and [Fig. 8] display a comparison of the computed mole fractions of reactants and of analyzed products with the experimental data at an equivalence ratio of 0.5. Fig. 7 also displays the computed and experimental evolutions with the temperature of the fuel consumption for the two other equivalence ratios, 0.5 and 1.5. A complete set of comparison (including all the experimental data obtained at $\phi = 1$ and $\phi = 1.5$) is provided as supplemental material (Figs. A-1 to A-6 in Appendix). At the three studied equivalence ratios, the fuel consumption predicted by the model generated with EXGAS is too rapid at low temperature and is in agreement with the experimental data only at temperatures higher than 850 K, whereas mole fractions of oxygen are well represented by our model. We did not find obvious reasons for the discrepancies in fuel consumption at low temperature under high pressure. They could be due to the fact that the pressure effects on complex reactions were not taken in account (for example, in our model, reactions of oxidation of alkyl radicals and reactions of addition of alkyl radicals to molecular oxygen are written in an independent manner, whereas these two reactions are likely connected through the formation of an intermediate chemically activated $ROO\bullet$ radicals).

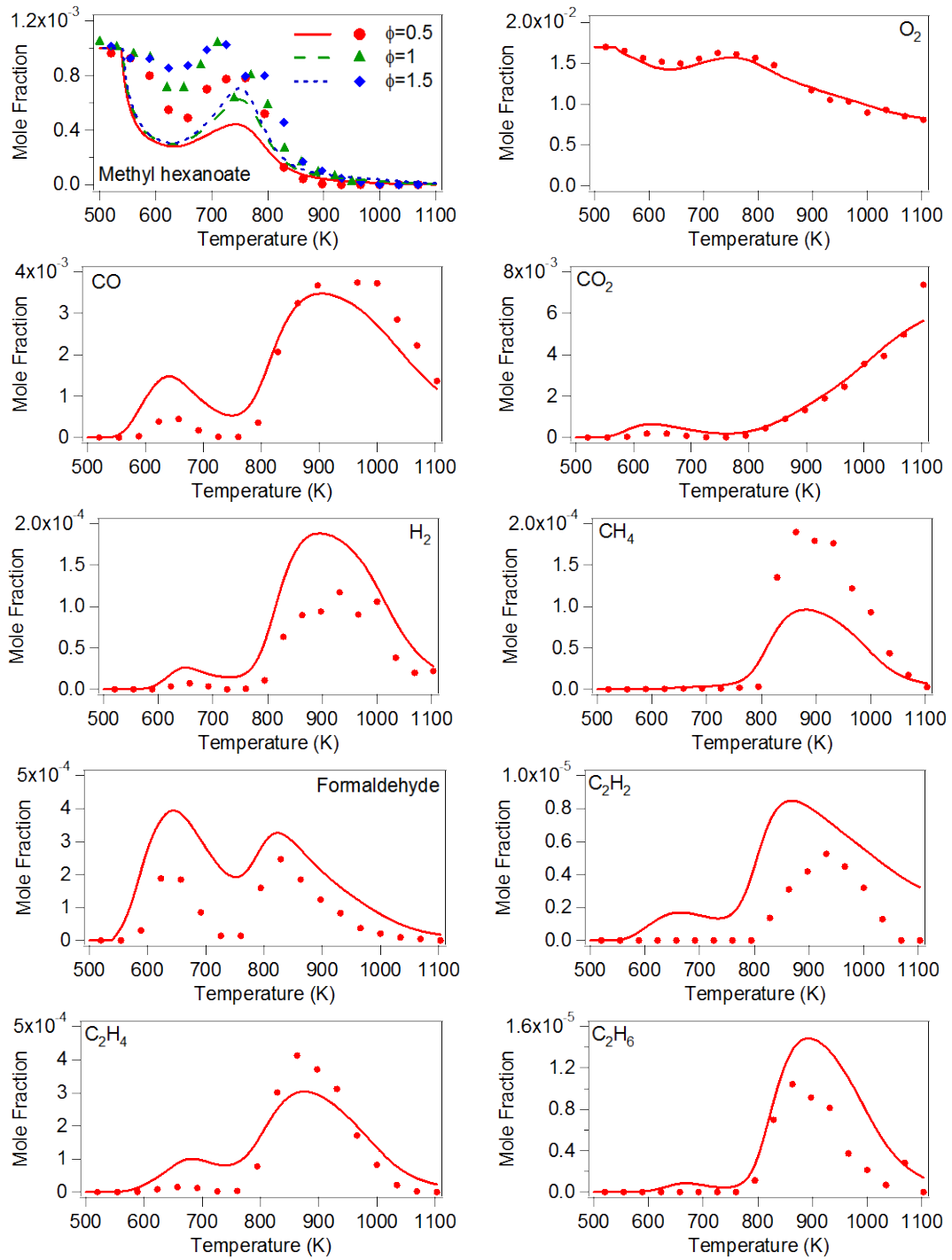


Fig. 7. Oxidation of methyl hexanoate in a jet-stirred reactor: comparison of the model with the experimental results obtained by Dayma et al. [16] (pressure: 10 atm, equivalence ratio: 0.5, inlet fuel mole fraction: 0.001, and residence time: 1 s). Part one.

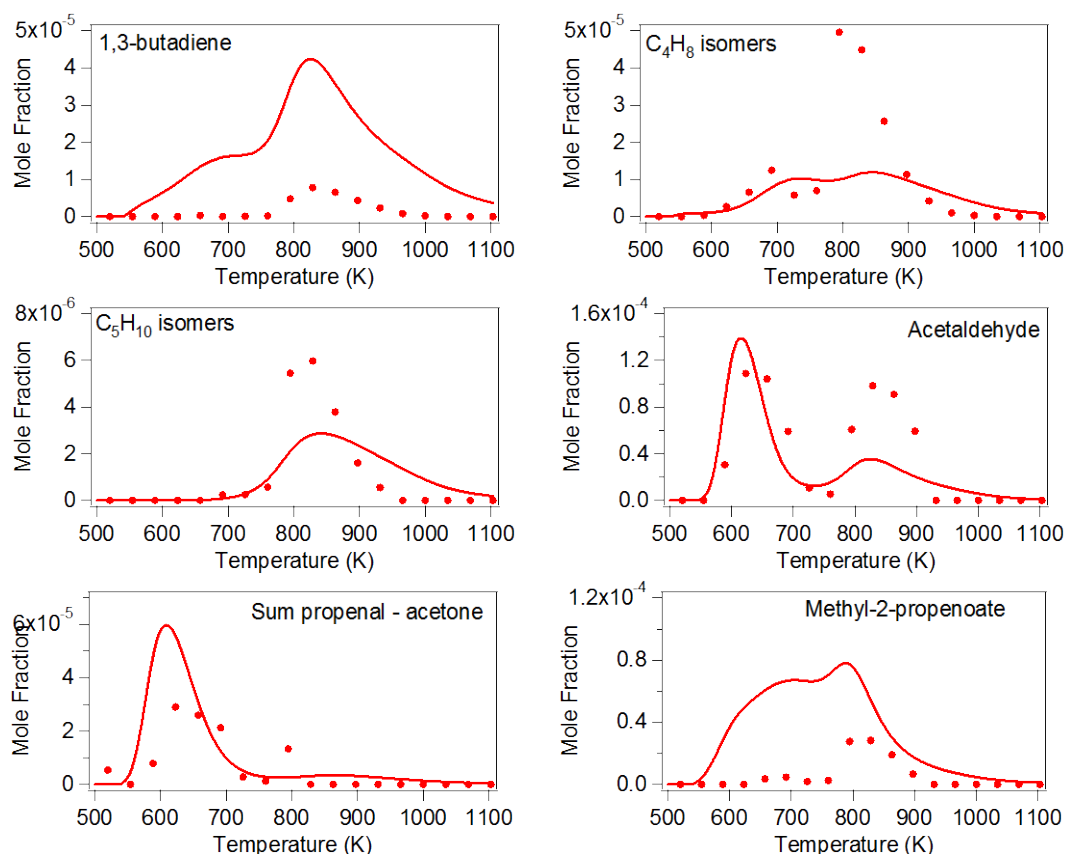


Fig. 8. Oxidation of methyl hexanoate in a jet-stirred reactor: comparison of the model with the experimental results obtained by Dayma et al. [16] (pressure: 10 atm, equivalence ratio: 0.5, inlet fuel mole fraction: 0.001, and residence time: 1 s). Part two.

As far as reaction products are concerned, the agreement is overall satisfactory. Computed mole fractions of some species are overpredicted at low temperature (e.g., CO, CH_2O , C_2H_4 , 1,3-butadiene, and methyl 2-propenoate). This is likely due to the over-prediction of the fuel consumption in this temperature range. In the case of 1,3-butadiene, the over-prediction can also be due to the chemical lumping of the reactions of consumption of large olefins and unsaturated esters which is responsible for the formation of large amounts of this species.

More recently, Dayma et al. [17] studied the oxidation of methyl heptanoate ($C_8H_{16}O_2$) in a jet-stirred reactor. Experiments were performed at a pressure of 10 atm, at a residence time of 0.7 s, at temperatures ranging from 550 to 1100 K, at three equivalence ratios, 0.6, 1, and 2, and at high dilution in nitrogen. Inlet fuel mole fraction was set to 0.001, as in the case of the methyl hexanoate study. Reaction products were analyzed by gas chromatography and FTIR. Species quantified in this study were oxygen, hydrogen, water, carbon monoxide, carbon dioxide, formaldehyde, methanol, methane, ethane, ethylene, propene, 1-butene, 1-pentene, and methyl heptanoate. Unsaturated esters and 1-hexene, the formation of which was expected, were not quantified.

A model for the oxidation of methyl heptanoate (531 species and 3236 reactions) was generated by the version of EXGAS described in this paper. [Fig. 9] and [Fig. 10] display a comparison of the computed evolutions with the temperature of the mole fractions of reactants and the analyzed products computed with the experimental data at of Dayma et al. [17] at an equivalence ratio of 1. A complete set of comparison (including all the experimental data obtained at $\phi = 0.6$ and $\phi = 2$) is provided as supplemental material (Fig. A-7 to A-10 in Appendix). As it was already the case for methyl hexanoate, the model generated with EXGAS over-predicts the consumption of the fuel at low temperature. The overall agreement is satisfactory for other species.

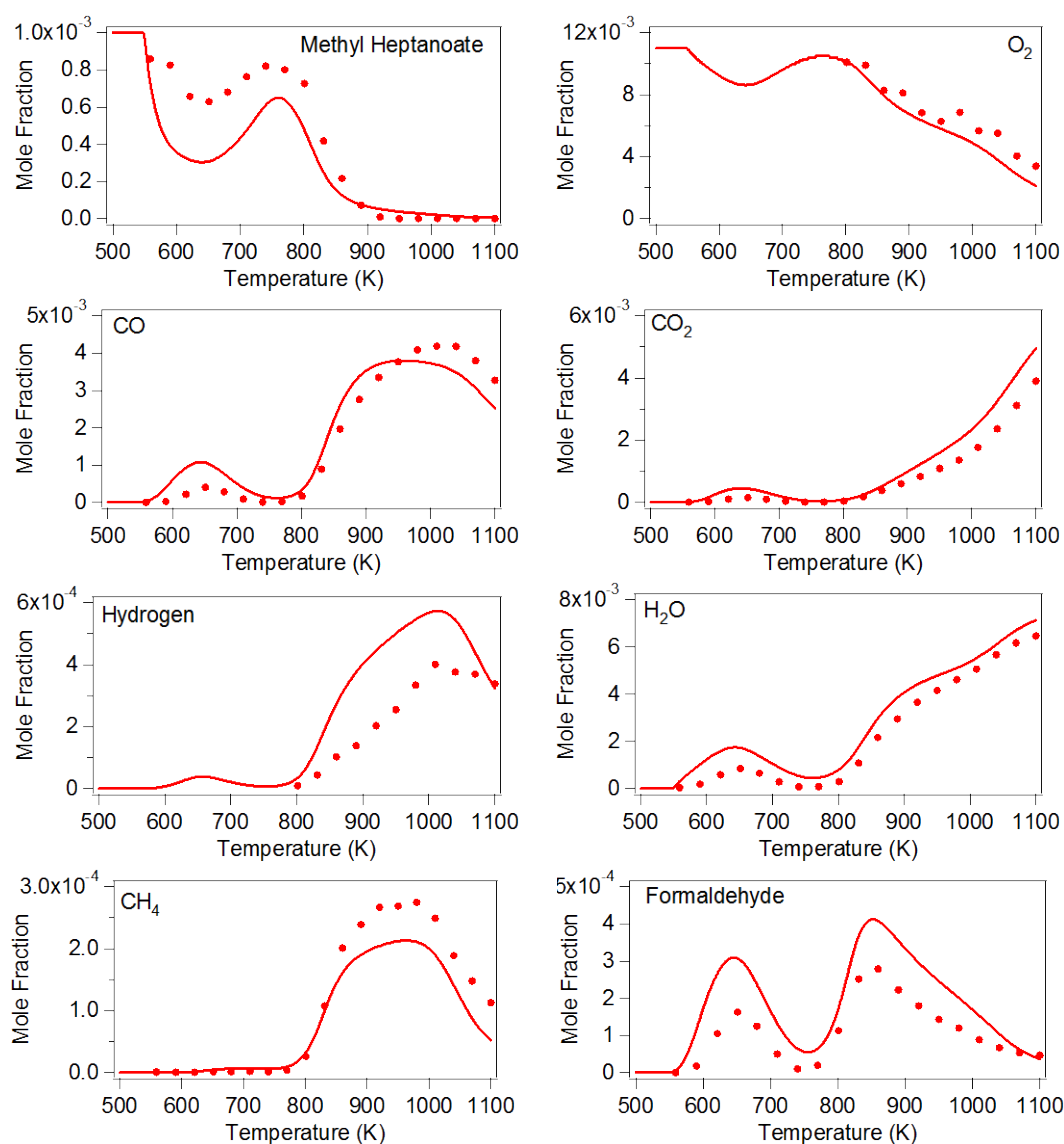


Fig. 9. Oxidation of methyl heptanoate in a jet-stirred reactor: comparison of the model with the experimental results obtained by Dayma et al. [17] (pressure: 10 atm, equivalence ratio: 1, inlet fuel mole fraction: 0.001, and residence time: 0.7 s). Part one.

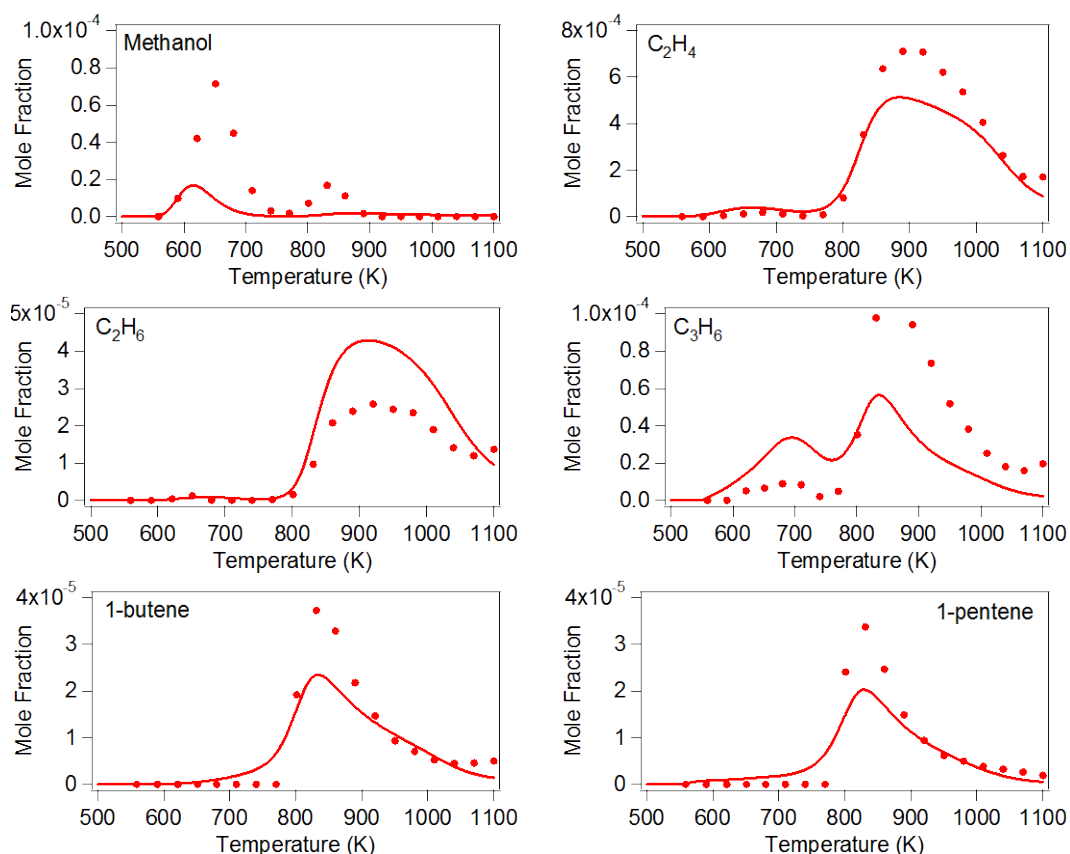


Fig. 10. Oxidation of methyl heptanoate in a jet-stirred reactor: comparison of the model with the experimental results obtained by Dayma et al. [17] (pressure: 10 atm, equivalence ratio: 1, inlet fuel mole fraction: 0.001, and residence time: 0.7 s). Part two.

5. Discussion

The new experimental results were also compared with simulations performed using the model proposed by Herbinet et al. [13] (see [Fig. 4], [Fig. 5] and [Fig. 6]). The agreement is also rather satisfactory. The model reproduces very well the conversion of the fuel and the mole fractions of oxygen and of many products. The main deviations are obtained for unsaturated species, such as 1-alkenes or unsaturated species, which are overestimated below 800 K. The predictions of cyclic ethers are very close to those made using our model. As far as the species distribution is concerned, it is difficult to compare the performance of both models as the secondary mechanisms were built in very different ways (in the LLNL model, decomposition reactions of molecules were not lumped, reactions being written by considering only the main decomposition paths). The main differences are lying in the way their decomposition is considered. The fate of this type of compounds has been very little studied and it would be interesting to look at them closely to revise this part of the model. There are no data in the literature about the effect of the ester group on the rate constant of the oxygen addition on the radical center borne in the α position of the carbonyl group. It is then difficult to explain why the formation of some cyclic ethers was not observed in the methyl decanoate experiments. More investigations are needed to clarify this point.

Flow rate analyses for the oxidation of n-decane and methyl decanoate at 650 K in the conditions of the methyl decanoate experiments in a jet-stirred reactor are displayed in Fig. 11. Note that our model and that of Herbinet et al. [13] have both been written using rules very close to those used in the case of alkanes by both Livermore [37] and [38] and Nancy combustion groups [19] and [20]. That makes the conclusions of the flow rate analysis very close to those which have been already drawn for alkane oxidation, e.g., that of n-decane [20]. That can be clearly seen in Fig. 11, which compares flow rate analyses for methyl decanoate and n-decane computed under the same conditions. The main difference in the consumption routes of the two fuels is due to the presence of the two H-atoms in the α position of the ester function, which are more easily abstractable. As an example, at 650 K, under the conditions of the methyl decanoate study, the rate of abstraction of these two particular H-atoms is about three times higher than the rate of abstraction of two secondary H-atoms. The production of molecules including both cyclic ether and ester functions derives from the same sequence of reactions (H-abstraction, addition to oxygen, isomerization, decomposition of hydroperoxy-alkyl radicals) as in the case of the cyclic ethers obtained during the oxidation of alkanes. At high temperatures (above the NTC region), the formation of unsaturated esters occurs via the same sequence of reactions as that of alkenes, mainly H-abstractions followed by β -scission decompositions. However as shown in Fig. 11, the formation of cyclic ethers is slightly favored in the case of methyl esters compared to alkanes.

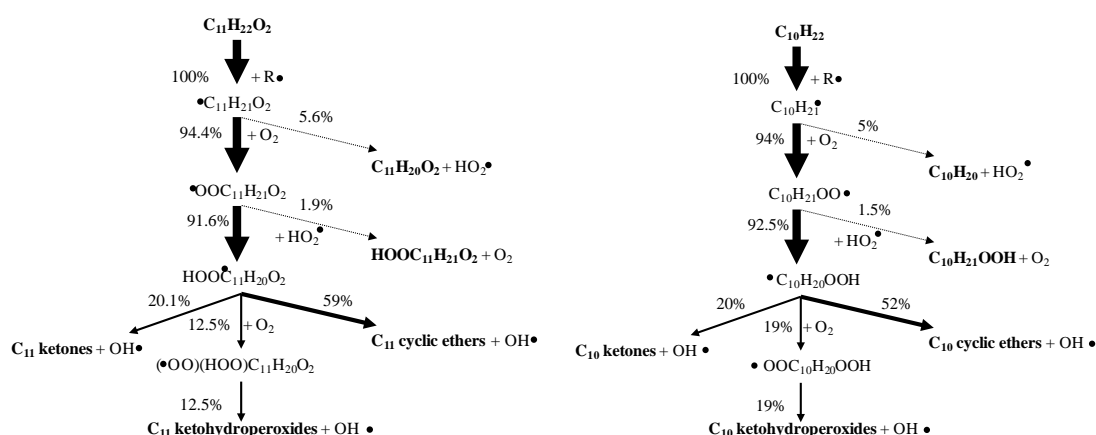


Fig. 11. Flow rate analyses for the oxidation of methyl decanoate ($C_{11}H_{22}O_2$) and n-decane ($C_{10}H_{22}$) in a jet-stirred reactor under the same conditions as the methyl decanoate experiments at 650 K.

Note that, as shown in Fig. 6, the formation of ether G is noticeably overestimated by our model and that of Herbinet et al. [13], and that the formation of the ethers F and F' (isomers), which was not experimentally observed, is predicted by both models. These two cyclic ether isomers derive either from the addition of oxygen to the alkyl radical obtained from the abstraction of a H-atom carried by the atom of carbon in the α position of the carbonyl group (31% of the formation at 650 K under the conditions of Fig. 6) or from the isomerization of a peroxy radical involving the abstraction of one of these two H-atoms (69% of the formation). The weakness of these C–H bonds favors the H-atom abstraction compared to those of the other H-atoms of the molecule (28% of the fuel consumption at 650 K).

Simulations performed under similar conditions showed that the three esters studied in this work have similar reactivities, methyl decanoate being the more reactive and methyl hexanoate being the least. Models generated with EXGAS predict that methyl octanoate and methyl nonanoate have reactivities lying in between. For esters larger than methyl decanoate, generated models lead to very close reactivities and there are almost no differences for the very large ones.

6. Conclusions

This paper presents the improvements which have been made to EXGAS-ALKANES [19] and [20] in order to also model the oxidation of ESTERS¹. This new software allows to generate models which can satisfactorily reproduce experimental data obtained in jet-stirred reactors over a wide range of temperature including the NTC zone, for methyl hexanoate, methyl heptanoate, and methyl decanoate.

For methyl decanoate, new experimental results have been obtained with the quantification of more than 30 reaction products, including unsaturated esters and cyclic ethers. For reproducing these results, our model for methyl decanoate and that of Herbinet et al. [13] do actually lead to the same level of agreement with slight differences in the product distribution due to the manner in which the secondary mechanisms were built. Models generated for methyl esters from C₇ to C₁₁ showed that these species have close reactivities under similar conditions, meaning that the size of the alkyl chain has almost no influence on the fate of the largest species. This study also showed that the ester group has very little influence on the reactivity of large esters and that this type of compounds reacts very similar to n-alkanes.

The modifications of the program EXGAS, made in order to handle methyl esters and to prove the ability of the generated models to correctly reproduce data about the oxidation of C₇, C₈, and C₁₁ methyl esters, open important perspectives in terms of modeling of larger compounds, such as methyl palmitate and methyl stearate, more representative of those actually present in biofuels.

Acknowledgments

This study was supported by the European Commission through a “Clean ICE” Advanced Research Grant from the European Research Council and by the ADEME in collaboration with the Institut

¹ Software EXGAS-ALKANES-ESTERS [39] automatically generates detailed kinetic mechanisms for the oxidation of linear and branched alkanes, and linear methyl esters and is freely available for academic researchers (valérie.warth@ensic.inpl-nancy.fr).

Français du Pétrole, PSA Peugeot Citroën, and TOTAL. We thank Professor R. Minetti, Dr. P. Dagaut, Dr. G. Vanhove, and Dr. G. Dayma for providing their experimental data before publication.

References

- [1] A.K. Agarwal, *Prog. Energy Combust. Sci.* 33 (2007), pp. 233–271.
- [2] M.S. Graboski and R.L. McCornick, *Energy Combust. Sci.* 24 (1998), pp. 125–164.
- [3] C.K. Westbrook, W.J. Pitz and H.J. Curran, *J. Phys. Chem. A* 110 (2006), pp. 6912–6922.
- [4] P. Pepiot-Desjardin, H. Pitsch, R. Malhotra, S.R. Kirby and A.L. Boehman, *Combust. Flame* 154 (2008), pp. 191–205.
- [5] J. Bünger, J. Krah, K. Baum, O. Schröder, M. Müller, G. Westphal, P. Ruhnau, T.G. Schulz and E. Hallier, *Arch. Toxicol.* 74 (2000), pp. 490–498.
- [6] A. Demirbas, *Prog. Energy Combust. Sci.* 31 (2005), pp. 466–487.
- [7] E.M. Fisher, W.J. Pitz, H.J. Curran and C.K. Westbrook, *Proc. Combust. Inst.* 28 (2000), pp. 1579–1586.
- [8] S. Gaïl, M.J. Thomson, S.M. Sarathy, S.A. Syed, P. Dagaut, P. Diévert, A.J. Marchese and F.L. Dryer, *Proc. Combust. Inst.* 31 (2007), pp. 305–311.
- [9] W.K. Metcalfe, S. Dooley, H.J. Curran, J.M. Simmie, A.M. El-Nahas and M.V. Navarro, *J. Phys. Chem. A* 111 (2007), pp. 4001–4014.
- [10] S. Dooley, H.J. Curran and J.M. Simmie, *Combust. Flame* 153 (2008), pp. 2–32.
- [11] S.M. Walton, M.S. Woolridge and C.K. Westbrook, *Proc. Combust. Inst.* 32 (2009), pp. 255–262.
- [12] M.H. Hakka, H. Bennadji, J. Biet, M. Yahyaoui, V. Warth, L. Coniglio, P.A. Glaude, F. Billaud and F. Battin-Leclerc, *Int. J. Chem. Kinet.* 42 (2010), pp. 226–252.
- [13] O. Herbinet, W.J. Pitz and C.K. Westbrook, *Combust. Flame* 154 (2008), pp. 507–528.
- [14] K. Seshadri, T. Lu, O. Herbinet, S. Humer, U. Niemann, W.J. Pitz and C.K. Law, *Proc. Combust. Inst.* 32 (2009), pp. 1067–1074.
- [15] K. HadjAli, M. Crochet, G. Vanhove, M. Ribaucour and R. Minetti, *Proc. Combust. Inst.* 32 (2009), pp. 239–246.
- [16] G. Dayma, S. Gaïl and P. Dagaut, *Energy Fuel* 22 (2008), pp. 1469–1479.
- [17] G. Dayma, C. Togbé and P. Dagaut, *Energy Fuel* 23 (2009), pp. 4254–4268.

- [18] V. Warth, N. Stef, P.A. Glaude, F. Battin-Leclerc, G. Scacchi and G.M. Côme, *Combust. Flame* 114 (1998), pp. 81–102.
- [19] F. Buda, R. Bounaceur, V. Warth, P.A. Glaude, R. Fournet and F. Battin-Leclerc, *Combust. Flame* 142 (2005), pp. 170–186.
- [20] J. Biet, M.H. Hakka, V. Warth, P.A. Glaude and F. Battin-Leclerc, *Energy Fuel* 22 (2008), pp. 2258–2269.
- [21] P.A. Glaude, F. Battin-Leclerc, R. Fournet, V. Warth, G.M. Côme and G. Scacchi, *Combust. Flame* 122 (2000), pp. 451–462.
- [22] P.A. Glaude, F. Battin-Leclerc, B. Judenherc, V. Warth, R. Fournet, G.M. Côme, G. Scacchi, P. Dagaut and M. Cathonnet, *Combust. Flame* 121 (2000), pp. 345–355.
- [23] S. Touchard, R. Fournet, P.A. Glaude, V. Warth, F. Battin-Leclerc, G. Vanhove, M. Ribaucour and R. Minetti, *Proc. Combust. Inst.* 30 (2005), pp. 1073–1081.
- [24] P. Barbé, F. Battin-Leclerc and G.M. Côme, *J. Chim. Phys.* 92 (1995), pp. 1666–1692.
- [25] H.A. Gueniche, P.A. Glaude, G. Dayma, R. Fournet and F. Battin-Leclerc, *Combust. Flame* 146 (4) (2006), pp. 620–634.
- [26] P.A. Glaude, W.J. Pitz, M.J. Thomson and R. Pitz, *Proc. Combust. Inst.* 30 (1) (2005), pp. 1111–1118.
- [27] R.J. Kee, F.M. Rupley, J.A. Miller, *Chemkin II: A FORTRAN Chemical Kinetics Package for the Analysis of a Gas-phase Chemical Kinetics*, SAND89-8009B, Sandia Laboratories, 1993.
- [28] C. Muller, V. Michel, G. Scacchi and G.M. Côme, *J. Chim. Phys.* 92 (1995), pp. 1154–1177.
- [29] S.W. Benson, *Thermochemical Kinetics* (second ed.), Wiley, New York (1976).
- [30] A. El-Nahas, M.V. Navarro, J.M. Simmie, J.W. Bozzelli, H.J. Curran, S. Dooley and W. Metcalfe, *J. Phys. Chem. A* 111 (2007), pp. 3727–3739.
- [31] Y.R. Luo, *Handbook of Bond Dissociation Energies in Organic Compounds*, CRC Press, Boca Raton (2003).
- [32] A.M. Dean and J.W. Bozzelli, *Combustion chemistry of nitrogen*. In: W.C. Gardiner, Editor, *Gas-phase Combustion Chemistry*, Springer-Verlag, New York (2000).
- [33] K.B. Wiberg and R.F. Waldron, *J. Am. Chem. Soc.* 113 (1991), pp. 7697–7705.
- [34] M.J. Frisch et al. *Gaussian03, Revision B05*; Gaussian, Inc., Wallingford, CT, 2004.
- [35] M.H. Hakka, P.A. Glaude, O. Herbinet and F. Battin-Leclerc, *Combust. Flame* 156 (11) (2009), pp. 2129–2144.
- [36] S. Bax, M.H. Hakka, P.A. Glaude, O. Herbinet and F. Battin-Leclerc, *Combust. Flame* 157 (2010), pp. 1220–1229.

[37] H.J. Curran, P. Gaffuri, W.J. Pitz and C.K. Westbrook, *Combust. Flame* 114 (1–2) (1998), pp. 149–177.

[38] C.K. Westbrook, W.J. Pitz, O. Herbinet, H.J. Curran and E.J. Silke, *Combust. Flame* 156 (1) (2009), pp. 181–199.

[39] F. Battin-Leclerc, J. Biet, R. Bounaceur, G.M. Côme, R. Fournet, P.A. Glaude, X. Grandmougin, O. Herbinet, G. Scacchi, V. Warth, *EXGAS-ALKANES-ESTERS: A Software for the Automatic Generation of Mechanisms for the Oxidation of Alkanes and Esters*, LRGP, UPR CNRS 3349, 2010.